American Mineralogist, Volume 74, pages 573–585, 1989

Hydrothermal orthoamphibole-bearing assemblages from the Gåsborn area, West Bergslagen, central Sweden

Arend H. Damman
Institute of Earth Sciences, Free University, de Boelelaan 1085, 1081 HV Amsterdam, The Netherlands

Abstract

In the Gåsborn area, West Bergslagen, central Sweden, two mineral assemblages are found in conduit zones for hydrothermal fluids from which manganiferous iron ores were deposited: (1) an older assemblage consisting of quartz, albite, phengite, chlorite, and Zn- and Mn-bearing magnetite and (2) a younger, overprinting assemblage, consisting of biotite, cordierite, orthoamphiboles, cummingtonite, Zn- and Mn-free magnetite, hercynite, and corundum. The chemistry of biotite and coexisting orthoamphiboles that have developed along hydrothermal veins associated with a high-level anorogenic (A-type) granite varies with distance from the veins. This suggests that the replacement of the older assemblage by the younger took place under influence of hydrothermal fluids expelled from the veins.

The orthoamphibole compositions span the entire field from anthophyllite to sodium gedrite, indicating that they were formed at temperatures above the crest of the solvus of the anthophyllite-gedrite miscibility gap. The maximum temperature and lithostatic pressure during the formation of the hydrothermal vein system are estimated at 560 °C and 1.0 kbar. Orthoamphibole and coexisting biotite in the hydrothermal veins crystallized after quartz, plagioclase, and cordierite, suggesting that they were formed at a temperature of <560 °C and implying that the crest of the solvus of the anthophyllite-gedrite miscibility gap at 1.0 kbar must also lie below this temperature.

The relative fugacity of HF ($f'_{HF} = f_{HF}/f_{H_2O}$) varies between veins from $10^{-3.53}$ to $10^{-4.58}$ and the relative fugacity of HCl (f'_{HCl}, i.e., f_{HCl}/f_{H_2O}) varies from $10^{-1.68}$ to $10^{-2.60}$. In and along each hydrothermal vein, f'_{HF} is relatively constant, and the amount of F incorporated in coexisting orthoamphibole and biotite is controlled by their respective Mg and Fe contents. In and along each vein, f'_{HCl} decreases when going from the vein outward, and X_{Mg} [= Mg/(Mg + Fe^{2+})] values of coexisting orthoamphibole and biotite show a negative correlation with their respective Cl contents, suggesting that along each vein, variations in f'_{HCl} and X_{Mg} mutually influence one another.

The Mg and Fe contents of orthoamphibole and biotite appear to be controlled by the differences in f'_{HF} and f'_{HCl} between veins. Ba and Ti are preferentially incorporated into biotite and show a positive correlation with Cl. Mn is preferentially incorporated into the orthoamphiboles, but does not show a correlation with either Cl or F.

Introduction

In the Gåsborn area, West Bergslagen, central Sweden, the high-level Ostra Höjden granite (Damman, 1988a)—which is assumed (Damman, in preparation) to belong to the group of older granites of the Bergslagen district (Åberg et al., 1983a, 1983b; Oen et al., 1984; Baker, 1985; Billström et al., 1988)—is intruded into a pile of silicic metavolcanics with intercalated marbles, metacherts, metamorphosed mafic lavas, and a metamorphosed manganiferous iron ore horizon (Fig. 1). This volcanosedimentary succession belongs to the Upper Leptite–Hälleflinta and Slate Group of the Bergslagen supracrustal series (Oen et al., 1982).

A hydrothermal vein system associated with the granite is characterized by an estimated maximum temperature (T) of 560 °C, lithostatic pressure (P_l) of approximately 1.0 kbar, and a maximum fluid pressure in the veins (P_f) of 4 kbar (at T = 560 °C). With decreasing T, P_f rapidly drops to values below P_l (Damman, manuscript). The hydrothermal vein system consists predominantly of quartz + feldspar veins, some containing andalusite, sekaninaite (Fe-cordierite), biotite, muscovite, fluorite, and accessory oxides and sulfides. In one vein, sekaninaite and andalusite constitute over 90 vol% of the vein, which furthermore contains minor plagioclase, topaz, sillimanite, quartz, subsilicic sodium gedrite, biotite, and accessory oxides and sulfides (Damman, 1988a).

Under influence of the hydrothermal activity, marbles and included metavolcanite and metachert lenses (Ic, Fig. 1) are locally altered into garnet + pyroxene skarns containing minor calcic amphibole, epidote, phlogopite,

0003–004X/89/0506–0573$02.00

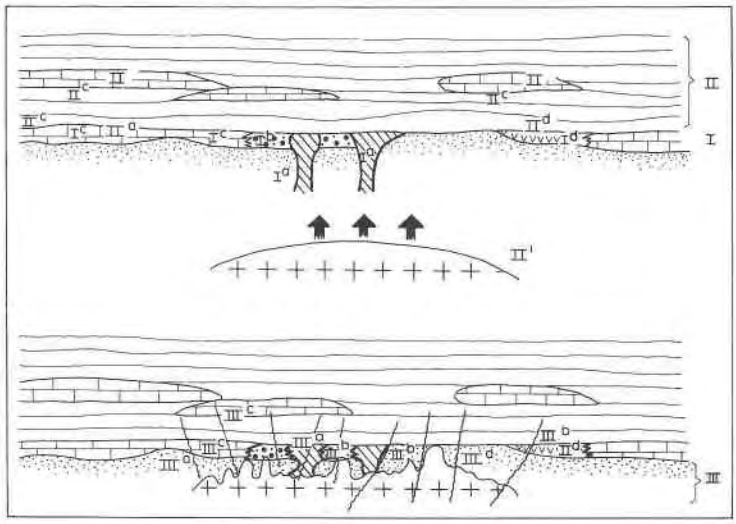

Fig. 1. A model for skarn formation and related processes in the Gåsborn area. **I**—deposition of the Gåsborn manganiferous iron ore horizon, consisting of (Damman, 1988b) (**Ia**) two feeder zones, containing Mn-poor iron ore–bearing magnesian metasomatically altered metavolcanics; (**Ib**) Mn-poor iron ore–bearing metavolcanics; (**Ic**) Mn-poor iron ore–bearing marbles; (**Id**) manganiferous iron ore–bearing metavolcanics and metacherts, followed by deposition of metavolcanics and marbles overlying the manganiferous iron ore horizon (II). **II**—intrusion of the Ostra Höjden granite and subsequent formation of calc-silicate reaction skarns in marbles (**IIc**; Damman, in preparation) and manganese silicate reaction skarns in manganiferous iron ore–bearing metavolcanics and metacherts (**IId**; Damman, in preparation). IIa and IIb are not labeled because nothing happened during event II in the conduit zones or metavolcanics, respectively. **III**—emplacement of the Ostra Höjden granite and subsequent (**IIIa**) formation of orthoamphibole, cordierite, biotite, and cummingtonite in the Mg-enriched conduit zones for fluids from which the manganiferous iron ores were deposited (this paper); (**IIIb**) biotitization of metavolcanics; (**IIIc**; Damman, unpublished manuscript) formation of metasomatic infiltration skarns in marbles and manganiferous iron ore–bearing metavolcanics and metacherts (**IIId**; Damman, unpublished manuscript).

fluorite, scheelite, and sulfides and calcic amphibole + biotite + orthoamphibole schist (IIc and IIIc, Fig. 1); manganiferous iron ores (Id, Fig. 1) are altered into manganese silicate + magnetite + jacobsite skarns (IId and IIId, Fig. 1); and felsic metavolcanics (Ib, Fig. 1) are locally altered to biotite (IIIb, Fig. 1). Hydrothermal veins associated with the Ostra Höjden granite also cut across two earlier conduit zones for fluids from which manganiferous iron ores are deposited (Damman, 1988b; Ia, Fig. 1). This paper describes the petrography and mineral chemistry of the rocks in the conduit zones. Evidence will be presented that cordierite, biotite, orthoamphiboles, cummingtonite, hercynite, and corundum in these rocks were formed out of phengite, chlorite, quartz, and albite by metasomatic reactions coeval with the intrusion of the Ostra Höjden granite (IIIa, Fig. 1).

Table 1. Counting times and errors in microprobe analyses of minerals in the present study

	t (s)	2σ (%)
Si	15	6
Al	15	4
Ti	15	2
Fe	15	4
Mn	15	3
Mg	15	5
Zn	15	2
Ca	15	3
Na	15	4
K	15	3
Ba	25	3
Cl	15	1
F	49	10

Analytical procedures

Electron-microprobe analyses were made with a Cambridge Instrument Company Microscan 9 operated at an acceleration potential of 20 kV and a sample current of 25 nA. Raw data were corrected with the Mark 9 online ZAF computer program. Standards used were marialite (Cl), orthoclase (K), diopside (Ca, Si), ilmenite (Ti), rhodonite (Mn), fayalite (Fe), jadeite (Na), corundum (Al), and synthetic ZnO (Zn). F was measured at a sample current of 40 nA, using fluorite as a standard. Counting times (s) and analytical errors (2σ) are presented in Table 1.

Relative (see below) HF fugacities (f'_{HF}) and relative HCl fugacities (f'_{HCl}) of fluids with which biotite and orthoamphibole equilibrated were calculated by using a modification of the method of Munoz (1984), who suggested that, from electron-microprobe analyses, the fol-

lowing equations can be used to determine f_{H_2O}/f_{HF} and f_{H_2O}/f_{HCl} of fluids from which biotite equilibrated:

$$\log [f_{H_2O}/f_{HF}] = 2100/T\,(K) + IV(F) \quad (1)$$

$$IV(F) = 1.52X_{Mg} + 0.42X_{An} + 0.2X_{Sid} + \log (X_F/X_{OH}) \quad (2)$$

$$\log [f_{H_2O}/f_{HCl}] = 5151/T\,(K) + IV(Cl) \quad (3)$$

$$IV(Cl) = -5.01 - 1.93X_{Mg} - \log (X_{Cl}/X_{OH}), \quad (4)$$

where $X_{Sid} = ([6]X_{Al}/0.167) \times (1 - X_{Mg})$, $X_{An} = 1 - (X_{Mg} + X_{Sid})$, $X_{Mg} = Mg/(Mg + Fe^{2+})$, and $X_{OH} = 4 - X_F - X_{Cl}$. X_F and X_{Cl} are the values given for F and Cl (formula units) in Tables 5 and 7. IV(F) and IV(Cl)—the F and Cl intercept values—are single numerical values designed to express the relative degree of F and Cl enrichment in a mica corrected for the effects of Fe-F and Mg-Cl avoidance (Munoz, 1984).

The hydrothermal solution under whose influence the orthoamphibole and biotite were formed (see below) consists almost entirely of saline water, with only minor other elements. All orthoamphibole and biotite under discussion were formed at approximately the same pressure and temperature, implying that it can safely be assumed that f_{H_2O} between all hydrothermal veins in and among which orthoamphibole and biotite were formed (see below under petrographic descriptions) during orthoamphibole and biotite formation had similar values (= constant, or c), changing Equations 1 and 3 into $\log (c/f_{HF}) = 2100/T + IV(F)$ and $\log (c/f_{HCl}) = 5151/T + IV(Cl)$, respectively. Omitting the constant from these modified equations leads to the following relative fugacities of F (f'_{HF}) and Cl (f'_{HCl}):

$$\log f'_{HF} = -[2100/T + IV(F)],$$

or

$$f'_{HF} = 10^{-[2100/T + IV(F)]} \quad (1')$$

and

$$\log f'_{HCl} = -[5151/T + IV(Cl)],$$

or

$$f'_{HCl} = 10^{-[5151/T + IV(Cl)]}. \quad (3')$$

For reasons discussed below, a T of 530 °C (803 K) is used in the above calculations of f'_{HF} and f'_{HCl}.

Because Fe^{3+} can only be determined accurately by wet-chemical analysis (Guidotti, 1984), no attempt was made to calculate Fe^{3+} in biotite. According to Munoz (1984), the absence of Fe^{3+} in biotite may introduce a maximal positive error as large as 0.25 IV unit in calculations of IV(F) and thus most probably also in calculations of IV(Cl), implying that all IV(F) and IV(Cl) values presented in this paper should be considered as maximal values. Analyses of orthoamphiboles discussed below suggest that only a small amount of Fe^{3+} is present in orthoamphibole. Biotite either occurs stably next to orthoamphibole or was formed slightly later, suggesting that the amount of Fe^{3+} in biotite is also very small.

Representative analyses of orthoamphiboles, biotite, magnetite, hercynite, and corundum are presented in Tables 2, 3, 4, 5, 7, and 8; structural formulae are calculated on the basis of 23 oxygens for amphiboles, 22 oxygens for biotite, 4 oxygens for magnetite and hercynite, and 3 oxygens for corundum. Total tetrahedral Si + Al is constrained to equal 8 in calculations of biotite and amphiboles. Several analyses of orthoamphibole (Tables 2, 4, and 8) show a total of slightly more than 7 cations in the M1–M4 sites. Forcing these analyses to 7 (Robinson et al., 1982) requires that a maximum of about 0.0065 Fe^{3+} should be present in the orthoamphiboles. According to Robinson et al. (1982), a good orthoamphibole analysis has about 0.08 Na in the M4 site. A recalculation of the orthoamphibole analyses presented in Tables 2, 4, and 8 for 0.08 Na in the M4 site suggests that, according to Robinson et al. (1982), 0.02 (+0.0065) Fe^{3+} should be present in the orthoamphiboles.

The suggestion of Robinson et al. (1982) is opposed by Berg (1985), who suggested that Fe^{3+} can be neglected, implying that in his calculations the only Na present in the M4 site is that amount necessary to force the sum of the cations in the M1–M4 sites to 7 (see below). As most of the analyses presented in Tables 2, 4, and 8 as well as the P-T conditions of orthoamphibole formation (Table 6) are relatively close to those of Berg, his suggestions are considered valid for the Gåsborn area, and no attempt was made to recalculate Na in M4 and consequently Fe^{3+}.

In orthoamphiboles with a total of less than 7 cations in the M1–M4 sites, Na is transferred from the A site to the M4 site, following the procedure of Berg (1985).

Petrography of the rocks in the conduit zones

The conduit zones at the derelict Gustav and Jacob Pers iron mines (Magnusson, 1930) occur at a 200-m distance from one another in the Gåsborn area (Damman, 1988b). Magnusson (1930) described the wall rocks of the ore bodies in these mines as a metavolcanic gneiss (in this paper referred to as metavolcanite), locally altered into cordierite + gedrite quartzite. The ore bodies consist of magnetite- and spinel-rich biotite + chlorite + orthoamphibole "skarn," crosscut by numerous quartz + feldspar veinlets. Samples for the present study were collected from dumps and outcrops surrounding the mines.

The fine- to medium-grain metavolcanites around the ore bodies show a granoblastic texture and consist of albite (35–50 vol%), quartz (30–40 vol%), and microcline (5–10 vol%). Locally 10–15 vol% biotite, cummingtonite replaced by calcic amphibole, cordierite, andalusite, and opaque minerals are also present. Biotite, cummingtonite, calcic amphibole, cordierite, and andalusite occur as up to 400-μm subhedral poikiloblasts, enclosing quartz and feldspars. The opaque minerals occur as tiny grains intergrown with biotite.

The cordierite + gedrite quartzite (Magnusson, 1930)

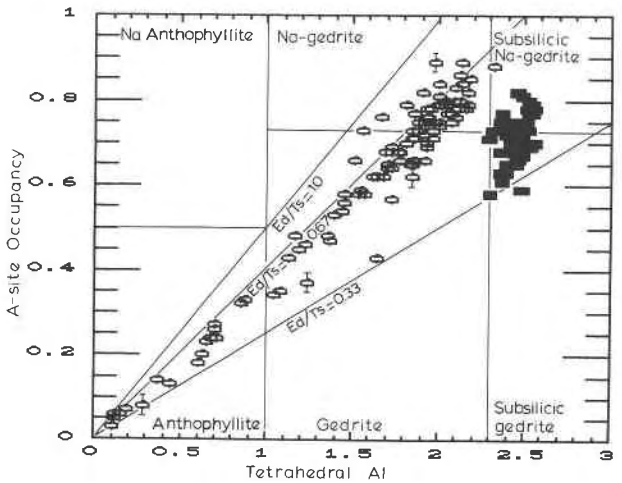

Fig. 2. ^{A}(Na + K) vs. $^{[4]}$Al for all orthamphiboles analyzed in the Gåsborn area; open symbols, this paper; filled symbols, Damman, 1988a. Edenite (Ed) substitution: Na (A) + $^{[4]}$Al = $\square_A$ + Si; tschermakite (Ts) substitution: $^{[4]}$Al + $^{[6]}$Al = Mg + Si.

shows a fine- to medium-grained matrix of quartz, albite, chlorite, phengite, magnetite, and ilmenite enclosed by aggregates of orthoamphibole, cordierite, and biotite. Quartz and albite occur as up to 50-μm anhedral crystals. Chlorite occurs as up to 200-μm colorless, anhedral crystals, and phengite occurs as up to 20-μm anhedral crystals intergrown with chlorite. Chlorite and phengite replace quartz and albite.

The orthoamphiboles, which vary in composition from anthophyllite to sodium gedrite (Table 2 and Fig. 2) occur as up to 500-μm subhedral crystals, replacing quartz, albite, phengite, and chlorite. The most Si-rich and Al-poor orthoamphiboles (analyses 1 and 2, Table 2) occur where biotite is absent. Orthoamphiboles coexisting with biotite become more Na- and Al-rich and Si-poor with increasing amounts of biotite and decreasing amounts of quartz and albite present. With quartz and albite present, the orthoamphibole compositions (analyses 1–6, Table 2) fall in the fields of anthophyllite and gedrite (Leake, 1978, Fig. 2). Sodium gedrite (analyses 7 and 8, Table 2) intergrown with biotite is only found where quartz and albite are absent. Cordierite occurs as up to 500-μm anhedral crystals, always intergrown with orthoamphibole and biotite. Biotite occurs as up to 200-μm pale brown and pale green pleochroic crystals, intergrown with orthoamphibole and cordierite.

Magnetite, occurring as tiny crystals in the quartz- and albite-bearing rocks, is characterized by small amounts of Zn and Mn (analysis 1, Table 3). Magnetite in rocks without quartz and albite is free of Zn and Mn (analysis 2, Table 3) and frequently shows coronitic rims of intergrown hercynite and corundum (analyses 3 and 4, Table 3). Locally, the coronitic rims contain small relict chlorite crystals. Magnetite of both described types often contain ilmenite lamellae and tiny inclusions of chalcopyrite and pyrrhotite.

The magnetite- and spinel-rich biotite + chlorite + orthoamphibole skarn of Magnusson (1930) contains four assemblages bearing cummingtonite + orthoamphibole + biotite that have minerals similar to those in the cordierite + gedrite quartzite, but with higher proportions of magnetite; the magnetite contents increase from the outer toward the inner parts of the ore bodies.

Where hydrothermal veins associated with the Ostra Höjden granite cut across the central parts of the ore bodies, a variation in the composition of biotite and the orthoamphiboles is found with distance (on the order of centimeters) from the hydrothermal veins. Where most perfectly developed, the following chemical variation is shown by orthoamphiboles and biotite in and around the hydrothermal veins: (1) The veins consist of quartz and feldspars with locally some cordierite and pale blue-brown pleochroic anthophyllite (analyses 3 and 4, Table 4) intergrown with dark brown pleochroic biotite, with relatively high amounts of Fe, Mn, Cl, Ba, and Ti (analyses 1 and 2, Table 5). Anthophyllite and biotite replace quartz, feldspars, and, if present, cordierite. (2) At the contact of veins and wall rock, a thin rim of pale blue pleochroic, up to 700-μm, subhedral anthophyllite (analyses 1 and 2, Table 4) is developed. (3) In the wall rocks near the hydrothermal veins, a more Na- and Al-rich gedrite (analyses 5 and 6, Table 4) than that in the veins is found intergrown with less Fe-, Mn-, Cl-, Ba-, and Ti-rich biotite than that in the veins (analyses 3 and 4, Table 5). (4) With increasing distance from the veins, gedrite becomes progressively enriched in Na, Al, and F and depleted in Fe and Si (analyses 6–8, Table 4); the color of the intergrown biotites changes from pale brown to pale green pleochroic, and they become progressively depleted in Fe, Cl, Ba, and Ti, and enriched in Mg and F (analyses 6–8, Table 5).

Formation of the orthoamphibole-bearing assemblages

The rocks described in this paper show a relict older assemblage consisting of quartz, albite, magnetite, phengite, and chlorite, which is replaced by a younger assemblage consisting of biotite, orthoamphiboles, cordierite, cummingtonite, a second magnetite, hercynite, and corundum. Damman (1988b) suggested that the relict older assemblage was formed by magnesian metasomatic alteration of metavolcanics in two conduit zones for hydrothermal fluids from which overlying manganiferous iron ores were deposited. The formation of orthoamphibole, cordierite, and biotite at the expense of chlorite, phengite, quartz, and albite may occur according to metamorphic reactions such as (1) chlorite + quartz = orthoamphibole + cordierite (Akella and Winkler, 1966) and (2) phengite + chlorite = biotite + cordierite (Helmers, 1984). However, biotite and orthoamphibole in and along the hydrothermal veins associated with the Ostra Höjden granite show rapid changes in Ti, Ba, Mn, Fe, Mg, F, and Cl contents with distance from the veins (Tables 4 and 5), suggesting that the orthoamphibole-, biotite-, and cor-

TABLE 2. Chemical analyses of anthophyllite, gedrite, and sodium gedrite from the outer parts of the conduit zones

	Anthophyllite			Gedrite		Sodium gedrite		
	1 H25.8	2 H25.7	3 H25.14	4 H25.13	5 H25.17	6 H25.10	7 H25.1	8 H25.3
SiO_2	52.02	51.47	48.32	46.60	43.87	41.94	39.27	38.94
Al_2O_3	2.73	4.37	6.15	9.62	12.29	16.06	19.31	19.61
TiO_2	0.07	0.07	0.13	0.17	0.22	0.17	0.33	0.35
FeO	24.92	25.24	24.95	24.82	25.08	24.20	21.10	21.50
MnO	0.25	0.27	0.21	0.27	0.31	0.39	0.40	0.37
MgO	16.33	15.84	14.96	14.29	12.54	12.47	13.04	13.02
CaO	0.22	0.22	—	0.32	0.34	0.61	0.37	0.36
Na_2O	0.35	0.61	0.80	1.19	1.80	2.36	3.05	2.94
F	0.17	0.19	0.18	0.29	0.47	0.20	0.20	0.21
Total	97.06	98.28	95.70	97.57	96.92	96.40	97.07	97.30
Si	7.72	7.56	7.32	6.94	6.64	6.24	5.87	5.81
$^{[4]}Al$	0.28	0.44	0.68	1.05	1.36	1.76	2.13	2.19
$^{[6]}Al$	0.20	0.32	0.42	0.64	0.83	1.06	1.27	1.26
Ti	0.01	0.01	0.01	0.02	0.02	0.02	0.04	0.04
Fe	3.09	3.10	3.16	3.09	3.17	3.01	2.64	2.68
Mn	0.03	0.03	0.03	0.03	0.04	0.05	0.05	0.05
Mg	3.61	3.47	3.38	3.18	2.83	2.76	2.90	2.90
Ca	0.04	0.03	—	0.05	0.06	0.10	0.06	0.06
Na	0.10	0.17	0.24	0.34	0.53	0.68	0.88	0.85
F	0.08	0.09	0.08	0.14	0.23	0.10	0.10	0.10
Total	15.16	15.22	15.32	15.48	15.71	15.78	15.94	15.94
^{A}Na	0.08	0.13	0.24	0.34	0.48	0.68	0.84	0.84
X_{Mg}	0.54	0.53	0.52	0.51	0.47	0.48	0.52	0.52
$^{A}Na/^{[4]}Al$	0.29	0.30	0.33	0.33	0.35	0.38	0.40	0.38
Ed/Ts	0.40	0.42	0.55	0.48	0.54	0.63	0.65	0.66

dierite-forming reactions took place under influence of hydrothermal fluids expelled from the veins, or, in other words, they were formed by high-temperature metasomatic reactions.

Hercynite and corundum are always associated with magnetite, biotite, and orthoamphiboles where the conduit zones do not contain any quartz or feldspars. This suggests that the formation of biotite and orthoamphibole at the expense of quartz, albite, phengite, and chlorite is related to the formation of hercynite and corundum. Magnetite occurring where the conduit zones contain quartz and albite frequently contains small amounts of Zn and Mn (analysis 1, Table 3), while magnetite rimmed by intergrown hercynite and corundum is free of these elements (analysis 2, Table 3). The rims of hercynite and corundum sometimes contain small relict chlorite fragments. On the basis of the above observations, the following reaction is proposed for the formation of hercynite and corundum: Zn- and Mn-bearing magnetite + some Mg and Al derived from the breakdown of chlorite = Zn- and Mn-free magnetite + hercynite + corundum.

ESTIMATION OF *P-T* CONDITIONS DURING FORMATION OF THE ORTHOAMPHIBOLE-BEARING ASSEMBLAGES

Damman (1988a) estimated the maximum temperatures and pressures of formation of the hydrothermal vein system associated with the Ostra Höjden granite at 550–600 °C and less than 3 kbar. A fluid-inclusion study of the granite and the hydrothermal veins (Damman, in preparation) suggests maximum temperatures of emplacement around 560 °C, confirming the above T estimates, but the latter study also shows that the greatest lithostatic pressure was about 1.0 kbar and that maximum fluid pressures in the hydrothermal veins were around 4 kbar.

The orthoamphiboles in the veins crystallized relatively late (after quartz, feldspars, and cordierite), suggesting that they were formed at $T < 560$ °C. Several papers (Robinson et al., 1969, 1970, 1971; Ross et al., 1969) have reported a miscibility gap between anthophyllite and gedrite. Figure 2 shows that the orthoamphiboles pre-

TABLE 3. Chemical analyses of magnetite, hercynite, and corundum

	Magnetite		Hercynite	Corundum
	1 G2.1	2 G11.Mt	3 G11.HCT	4 G11.Cor
SiO_2	0.35	—	—	—
Al_2O_3	0.32	0.35	58.49	98.09
Fe_2O_3	68.83	68.43	2.76	1.95
FeO	29.57	30.77	31.48	—
MnO	0.22	—	0.53	—
MgO	—	—	5.74	—
ZnO	0.34	—	1.86	—
Total	99.73	99.55	100.85	100.14
Si	0.01	—	—	—
Al	0.02	0.02	1.94	1.98
Fe^{3+}	1.99	1.98	0.06	0.02
Fe^{2+}	0.96	1.00	0.74	—
Mn	0.01	—	0.01	—
Mg	—	—	0.24	—
Zn	0.01	—	0.04	—
Total	3.00	3.00	3.03	2.00

Note: Analysis 1 is of magnetite that occurs without hercynite or corundum. Analysis 2 is of magnetite that occurs with hercynite (analysis 3) and corundum (analysis 4).

Table 4. Variation in orthoamphibole chemistry with distance from the hydrothermal veins in the central part of the conduit zones

	Anthophyllite				Gedrite		Sodium gedrite			
	1 G11.9	2 G11.7	3 G11.1	4 G11.2	5 G11.11	6 G11.10	7 G11.15	8 G11.17	9 G11.26	10 G11.27
SiO_2	52.39	51.91	48.33	48.19	41.87	40.61	39.06	40.10	40.53	40.08
Al_2O_3	1.26	1.38	5.99	6.04	14.25	16.29	18.99	18.76	18.17	18.72
TiO_2	—	—	0.33	0.33	0.42	0.22	—	—	0.11	—
FeO	28.44	29.37	28.68	28.85	26.06	25.70	22.43	22.87	20.68	20.62
MnO	0.62	0.54	1.28	1.14	0.84	0.84	0.73	0.69	—	—
MgO	13.79	13.16	12.22	11.98	11.01	10.96	12.10	12.97	14.22	13.76
CaO	0.29	0.23	0.21	0.23	0.59	0.51	0.43	0.40	0.55	0.49
Na_2O	0.23	0.25	1.03	0.99	2.15	2.25	2.78	2.79	2.78	2.68
Cl	0.02	0.03	0.07	0.10	0.05	0.03	0.03	0.03	—	—
F	0.16	0.12	0.06	0.13	0.28	0.25	0.34	0.33	0.40	0.42
Total	97.20	96.99	98.20	97.98	97.62	97.66	96.89	98.94	97.44	96.77
Si	7.89	7.88	7.30	7.30	6.36	6.16	5.90	5.92	6.01	5.98
$^{[4]}Al$	0.11	0.12	0.70	0.70	1.64	1.84	2.10	2.08	1.99	2.02
$^{[6]}Al$	0.12	0.13	0.37	0.38	0.93	1.07	1.28	1.19	1.19	1.27
Ti	—	—	0.04	0.04	0.05	0.03	—	—	0.01	—
Fe	3.60	3.74	3.62	3.66	3.31	3.26	2.83	2.82	2.56	2.57
Mn	0.08	0.07	0.16	0.15	0.11	0.11	0.09	0.09	—	—
Mg	3.11	2.98	2.75	2.71	2.49	2.48	2.72	2.86	3.14	3.06
Ca	0.05	0.04	0.03	0.04	0.09	0.08	0.07	0.06	0.09	0.08
Na	0.07	0.07	0.30	0.29	0.63	0.66	0.81	0.80	0.80	0.77
Cl	0.01	0.01	0.03	0.05	0.02	0.01	0.01	0.01	—	—
F	0.08	0.06	0.03	0.06	0.14	0.12	0.17	0.16	0.20	0.21
Total	15.03	15.03	15.27	15.27	15.61	15.69	15.80	15.82	15.79	15.75
^{A}Na	0.03	0.03	0.27	0.27	0.63	0.66	0.80	0.80	0.79	0.75
X_{Mg}	0.46	0.44	0.43	0.43	0.43	0.43	0.49	0.50	0.55	0.54
$^{A}Na/^{[4]}Al$	0.27	0.25	0.38	0.38	0.38	0.36	0.38	0.38	0.39	0.37
Ed/Ts	0.38	0.33	0.63	0.63	0.62	0.56	0.62	0.63	0.66	0.59

sented in this paper show a complete range of A-site and $^{[4]}Al$ values of 0.02–0.89 and 0.10–2.32, respectively, implying that they were formed under supersolvus conditions (for discussion of data, see below under orthoamphibole chemistry). Crowley and Spear (1981) and Robinson et al. (1982) suggested that, with respect to A-site occupancy, the miscibility gap widens and the temperature of the crest of the solvus increases, going from Mg-rich to Fe-rich bulk compositions.

Crowley and Spear (1981) also suggested that the slope of the critical curve for the solvus has a positive dP/dT. The orthoamphiboles presented in this paper were formed at $T < 560$ °C, implying that the temperature of the crest of the solvus of the anthophyllite-gedrite miscibility gap must also be below 560 °C at 1.0 kbar and X_{Mg} values of the orthoamphibole between 0.35 and 0.62 (Fig. 3; for discussion of data, see below under orthoamphibole chemistry). This result confirms the suggestion of Crowley and Spear (1981).

Orthoamphibole chemistry

In Figure 2, all orthoamphibole analyses made for the present study and some analyses of subsilicic sodium gedrite presented by Damman (1988a, see below) are plotted in a diagram of maximum occupancy of Na in the A site versus $^{[4]}Al$ (Berg, 1985); the orthoamphiboles show the largest variation in the ratios of Na in the A site to $^{[4]}Al$ ever reported for one single locality. Also shown in Figure 2 is the subdivision of the orthoamphiboles according to the nomenclature of Leake (1978).

The subsilicic sodium gedrite (Damman, 1988a; analyses 5 and 6, Table 8) presented in Figure 2 is found in a hydrothermal vein that belongs to the same hydrothermal vein system as the veins crosscutting the conduit zones described in this paper. Instead of crosscutting the rocks of the conduit zones that were already Mg enriched prior to hydrothermal vein formation (Damman, 1988b), however, this vein crosscuts Mg-poor metavolcanics several hundred meters away from the conduit zones (Damman, 1988a). The vein shows the following crystallization sequence (Damman, 1988a): andalusite, andalusite + cordierite, cordierite + subsilicic sodium gedrite, biotite, and quartz + albite + sillimanite + oxides + sulfides.

Robinson et al. (1971, 1982) and Spear (1980) showed a moderate inverse correlation between the edenite/tschermakite ratio [calculated as $^{A}(Na + K)/[^{[4]}Al - {}^{A}(Na + K)]$, see Berg (1985) and Fig. 2]. Berg (1985) showed a similar moderate inverse correlation between the $^{A}(K + Na)/^{[4]}Al$ ratio and X_{Mg}. These correlations suggest that the edenite/tschermakite ratio of orthoamphiboles is crystallographically and crystallochemically controlled by the incorporation of Mg and Fe in the M1–M3 sites of the orthoamphibole structure. In Figure 3, the orthoamphiboles analyzed for the present study and subsilicic sodium gedrite (Damman, 1988a) are plotted in an A-site occupancy per $^{[4]}Al$ vs. X_{Mg} diagram similar to that used by Berg (1985). This figure shows a wide variation in X_{Mg} and ratios of A-site occupancy to $^{[4]}Al$, but only shows a moderate positive correlation between them.

In Table 6 a comparison is made between P-T condi-

tions of formation and edenite/tschermakite ratios of orthoamphiboles analyzed for the present study, subsilicic sodium gedrite (Damman, 1988a), and orthoamphiboles from other localities derived from the literature. Although there is a large variation of *P-T* conditions and edenite/tschermakite ratios, it is interesting to notice that the orthoamphiboles with the highest edenite/tschermakite ratios (Berg, 1985; this paper) were formed at the lowest pressures, suggesting that a decrease in lithostatic pressure may favor the edenite substitution at expense of the tschermakite substitution, given that enough Na, Al, and Si to fulfill this condition are available (see below).

The subsilicic sodium gedrite (Damman, 1988a) was formed under the same *P-T* conditions as the orthoamphiboles in the conduit zones described in this paper, but shows much lower edenite/tschermakite ratios. The Si and Al content of the subsilicic sodium gedrite are controlled by those of coexisting cordierite, while its Na is derived from a hydrothermal fluid (Damman, 1988a). Biotite (analyses 5 and 6, Table 7) and subsilicic sodium gedrite (analyses 5 and 6, Table 8) from the subsilicic sodium gedrite–bearing hydrothermal vein are very rich in Fe and only contain minor Mg. The country rock around this vein does not contain these elements, suggesting that they are fluid derived and implying that the vein-forming fluid was relatively rich in Fe and did not contain much Mg. The data presented in Tables 4 and 5 show that orthoamphibole and biotite in hydrothermal veins crosscutting the conduit zones described in this paper are also relatively Fe rich (analyses 1–4, Table 4, and analyses 1 and 2, Table 5). Going from the veins into the country rock, these minerals change in composition from Fe rich to more Mg rich, suggesting that the Mg-enriched rocks of the conduit zones (Damman, 1988b) acted as a source of the Mg incorporated in orthoamphibole and biotite.

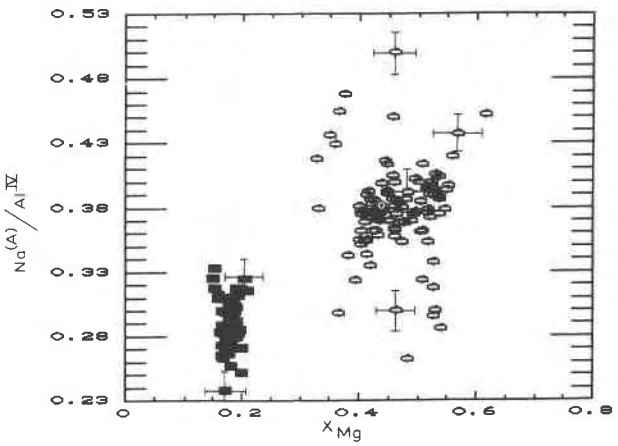

Fig. 3. A-site occupancy per $^{[4]}$Al vs. X_{Mg} for all orthoamphiboles analyzed in the Gåsborn area. For symbols, see Fig. 2.

TABLE 5. Variaton in biotite chemistry with distance from the hydrothermal veins in the central part of the conduit zones

	1 G11.1b	2 G11.3b	3 G11.4b	4 G11.5b	5 G11.7b	6 G11.10b	7 G11.18b	8 G11.19b
SiO_2	34.61	35.78	35.22	35.99	35.75	36.74	37.49	36.31
Al_2O_3	15.70	15.58	16.60	16.76	16.98	17.12	16.84	16.96
TiO_2	2.01	1.82	0.92	1.06	0.49	0.25	0.15	0.19
BaO	0.65	0.53	0.10	0.28	0.11	—	—	—
FeO	22.94	20.80	18.11	16.19	16.08	14.66	14.14	14.18
MnO	0.12	0.11	0.05	0.05	—	—	0.04	—
MgO	10.50	11.06	13.77	14.51	15.28	16.22	16.40	16.17
Na_2O	0.39	0.22	0.35	0.38	0.41	0.44	0.44	0.42
K_2O	8.59	9.30	9.34	9.56	8.26	8.95	8.88	9.07
Cl^-	0.93	0.70	0.27	0.25	0.18	0.19	0.16	0.17
F^-	0.70	0.79	0.86	0.91	0.96	1.01	1.13	1.70
Total	97.14	96.69	95.59	95.94	94.50	95.62	95.63	95.17
Si	5.39	5.54	5.41	5.46	5.45	5.51	5.59	5.50
$^{[4]}$Al	2.61	2.46	2.59	2.54	2.55	2.49	2.41	2.50
$^{[6]}$Al	0.27	0.38	0.41	0.46	0.50	0.54	0.55	0.53
Ti	0.24	0.21	0.11	0.12	0.06	0.03	0.02	0.02
Ba	0.04	0.03	0.01	0.02	0.01	—	—	—
Fe	2.99	2.69	2.32	2.05	2.05	1.83	1.77	1.80
Mn	0.02	0.01	0.01	0.01	—	0.01	—	—
Mg	2.44	2.55	3.15	3.28	3.47	3.63	3.64	3.65
Na	0.12	0.06	0.10	0.11	0.12	0.12	0.12	0.12
K	1.71	1.84	1.83	1.85	1.60	1.71	1.69	1.71
Cl	0.24	0.18	0.08	0.06	0.04	0.04	0.04	0.04
F	0.34	0.38	0.42	0.44	0.46	0.48	0.51	0.82
Total	16.41	16.32	16.44	16.49	16.31	16.39	16.39	16.69
X_{Mg}	0.45	0.49	0.58	0.62	0.63	0.66	0.67	0.67
X_{Sid}	0.15	0.19	0.17	0.17	0.19	0.18	0.18	0.17
X_{An}	0.40	0.32	0.25	0.21	0.18	0.16	0.15	0.16
IV(F)	1.88	1.87	1.94	1.96	1.95	1.96	1.91	1.69
log f'_{HF}	−4.50	−4.49	−4.56	−4.58	−4.57	−4.58	−4.53	−4.41
IV(Cl)	−4.73	−4.68	−4.49	−4.44	−4.29	−4.34	−4.37	−4.41
log f'_{HCl}	−1.68	−1.73	−1.92	−1.97	−2.12	−2.07	−2.04	−2.00

Table 6. A comparison of edenite/tschermakite ratios (Ed/Ts) and P and T of formation for orthoamphiboles from different localities

	Ed/Ts	P (kbar)	T (°C)
This paper	0.33–0.88	<1.5	<560
Damman (1988a)	0.31–0.50	<1.5	<560
Berg (1985)	0.54–0.86	2 ± 1	615
Otten (1984)	0.68	>5	500–550
Spear (1980)	0.05–0.50	>4	530
Abraham and Schreyer (1973)	approx. 0.33–0.63	0.5	550–580
Zotov and Siderenko (1967)	0.21	<11	?
James et al. (1978)	approx. 0.36–0.52	3–6	625
Lal and Moorehouse (1969)	0.26–0.27	<10	400–700
Kroonenberg (1976)	0.33	5–6	700–800

The above data suggest that besides X_{Mg} (Robinson et al., 1971, 1982; Spear, 1980; Berg, 1985), pressure and the paragenesis (or, in other words, the availability of Na, Al, Si, Mg, and Fe) have a large influence on edenite/tschermakite ratios and the X_{Mg} of orthoamphiboles. These data contradict the suggestions of Robinson et al. (1971, 1982), Spear (1980), and Berg (1985), who suggested that edenite/tschermakite ratios of orthoamphiboles are only crystallochemically controlled by their X_{Mg}.

F and Cl in orthoamphibole and biotite

Field, experimental, and theoretical data on F and Cl in biotite (reviews by Munoz and Ludington, 1974, 1977; Petersen et al., 1982; Valley et al., 1982; and Munoz, 1984) show that the extent of F incorporation in biotite depends on X_{Mg} [Mg/(Mg + Fe)], the amount of $^{[6]}$Al present in the biotite, and the HF fugacity (f_{HF}) during the formation of the biotite. The effect of X_{Mg} is discussed by Munoz and Ludington (1974, 1977), Petersen et al. (1982), Valley et al. (1982), and Munoz (1984) who showed that for any given ratio of f_{H_2O}/f_{HF} in fluids with which biotite equilibrates, the F/OH ratio in biotite increases with X_{Mg}.

Valley et al. (1982) discussed the effect of f_{HF} on the incorporation of F in biotite, and they showed that compared to Mg-rich biotites, Fe-rich biotites require a higher f_{HF} to stabilize a given amount of F. Valley et al. (1982) also suggested that at any ratio of f_{H_2O}/f_{HF} in fluids with which biotite equilibrates, an increase of the $^{[6]}$Al content enhances incorporation of F. The latter effect is opposed to the results of experiments of Munoz and Ludington (1974), who did not find any correlation between $^{[6]}$Al and F in annite and siderophyllite.

The small amount of Cl in biotite, commonly much lower than that of F, makes it difficult to evaluate the crystallochemical controls of its incorporation in biotite (Munoz, 1984). Leelanandem (1969) reported that Cl content in biotite containing 0.19 to 0.62 wt% Cl is not correlated with X_{Mg}. Jacobs (1976) reported biotites with 0.1–0.3 wt% Cl that show an increase in Cl content with increasing Fe contents; this suggests that incorporation of Cl in biotite at any given ratio of f_{H_2O}/f_{HCl} in fluids with which biotite equilibrates may be related to their Fe contents in a similar way as the incorporation of F is related to Mg. According to Munoz (1984) and Volfinger et al. (1985) this so-called Mg-Cl avoidance is confirmed by many analyses of natural biotites and amphiboles.

The few available data on F in orthoamphiboles led Berg (1985) to suggest that F incorporation in orthoamphibole is related to Mg contents, in a way similar to the case in biotite.

No published data on Cl in orthoamphibole could be found in the literature, and none of the orthoamphiboles described here contains over 0.10 wt% Cl.

To evaluate the above suggestions, biotite and orthoamphibole occurring in and along (maximal distance from the vein–wall rock contact = 20 cm) three hydrothermal veins associated with the Ostra Höjden granite, which crosscut the conduit zones described in this paper (Fig. 1), are plotted in diagrams of X_{Mg} vs. F (Fig. 4a), X_{Mg} vs. Cl (Fig. 4b), and $^{[6]}$Al vs. F (Fig. 4c) for biotite and in a diagram of X_{Mg} vs. F (Fig. 4d) for orthoamphibole. In the veins, biotite and coexisting orthoamphibole replace quartz, plagioclase, and, if present, cordierite. In the wall rock of the veins, biotite and orthoamphibole occur in intergrown masses, replacing quartz, albite, phengite, and chlorite, which were formed by magnesian metasomatic alteration of volcanics during deposition of the Gåsborn manganiferous iron ores (Fig. 1; Damman, 1988b). For comparison, biotite and subsilicic sodium gedrite from the subsilicic sodium gedrite–bearing vein described by Damman (1988a) are plotted as well. From the discussion presented in the section on analytical procedures, it follows that f'_{HF} and f'_{HCl} are used instead f_{H_2O}/f_{HF} and f_{H_2O}/f_{HCl}.

Chemical data on some orthoamphibole and biotite from one vein (marked with + signs in Figs. 4a–4d) are presented in Tables 4 and 5, and data on some orthoamphibole and biotite from the other veins and the subsilicic sodium gedrite–bearing vein are presented in Tables 7 and 8 and by Damman (1988a).

Tables 5 and 7 show that a considerable difference in f'_{HF} exists among the four hydrothermal veins under discussion, and they show that for each of the veins, when going from the vein outward (compare analyses 1 and 8, Table 5) f'_{HF} remains relatively constant. Tables 5 and 7 and Figure 4a show that biotites from different veins with similar X_{Mg} values have very different F contents, suggesting that these differences in F content are caused by the between-vein differences in f'_{HF} discussed above (Valley et al., 1982). Whenever biotite from a single vein and the surrounding country rock show a variation in X_{Mg}, X_{Mg} increases when going from the vein outward, and the F content of the biotite increases with increasing X_{Mg} (compare analyses 1–8 in Table 5 and Fig. 4a). These data suggest that in and along each vein, at more or less constant f'_{HF}, the F content of biotite is controlled by the effect of F-Fe avoidance (Munoz and Ludington, 1974, 1977; Petersen et al., 1982; Valley et al., 1982; Munoz, 1984).

TABLE 7. Analyses of biotite along two hydrothermal veins described in this paper (G32 and G23) and biotite (E7) described by Damman (1988a)

	G32.01	G32.02	G23.7	G23.6	E7.2	E7.3
SiO_2	34.75	35.73	37.85	38.48	35.81	36.17
Al_2O_3	17.36	17.13	15.91	15.51	17.30	17.36
TiO_2	1.09	1.05	0.06	0.02	0.30	0.65
BaO	—	—	—	—	—	—
FeO	19.31	19.26	14.57	14.94	22.76	20.90
MnO	0.04	—	0.09	0.05	0.21	0.15
MgO	12.61	12.50	15.72	16.17	8.78	10,42
Na_2O	0.20	0.16	0.85	0.90	0.56	0.71
K_2O	8.59	8.76	8.62	8.83	8.85	8.78
Cl^-	0.15	0.18	0.10	0.10	0.10	0.10
F	0.79	0.81	3.87	3.68	3.29	3.28
Total	94.89	95.55	97.64	98.68	97.96	98.52
Si	5.37	5.47	5.71	5.74	5.58	5.55
$^{[4]}Al$	2.63	2.53	2.29	2.26	2.42	2.45
$^{[6]}Al$	0.53	0.56	0.54	0.47	0.76	0.69
Ti	0.13	0.12	0.01	—	0.03	0.08
Ba	—	—	—	—	—	—
Fe	2.49	2.46	1.84	1.86	2.97	2.68
Mn	0.01	—	0.01	0.01	0.03	0.02
Mg	2.90	2.85	3.53	3.59	2.04	2.38
Na	0.06	0.05	0.25	0.26	0.17	0.21
K	1.69	1.71	1.64	1.68	1.76	1.72
Cl	0.04	0.04	0.02	0.02	0.02	0.02
F	0.39	0.39	1.86	1.74	1.62	1.59
Total	16.24	16.18	17.69	17.64	17.40	17.40
X_{Mg}	0.54	0.53	0.66	0.66	0.40	0.47
X_{Sid}	0.24	0.26	0.18	0.16	0.46	0.37
X_{An}	0.22	0.21	0.16	0.18	0.14	0.16
IV(F)	1.92	1.90	1.16	1.21	0.91	1.03
log f'_{HF}	−4.54	−4.51	−3.80	−3.84	−3.53	−3.64
IV(Cl)	−4.10	−4.08	−4.34	−4.32	−3.81	−3.94
log f'_{HCl}	−2.31	−2.33	−2.07	−2.09	−2.60	−2.47

Tables 5 and 7 show that f'_{HCl} of the fluid with which biotite equilibrated also varies considerably between veins. Table 5 shows that f'_{HCl} decreases when going from a hydrothermal vein outward (compare analyses 1 and 8). The X_{Mg} vs. Cl plot (Fig. 4b) shows that biotites with similar X_{Mg} values from different hydrothermal veins have different Cl contents, and it shows that whenever a variation in X_{Mg} of biotite along a single vein exists (Table 5), €l shows a negative correlation with X_{Mg}. The above data suggest that (1) between veins, incorporation of Cl in biotite is controlled by variation of f'_{HCl} and (2) along each vein, the variation in f'_{HCl} and the effect of Mg-Cl avoidance (Munoz, 1984; Volfinger et al., 1985) mutually influence one another.

The plot of $^{[6]}Al$ vs. F (Fig. 4c) shows a wide range of F content and a much smaller range in $^{[6]}Al$ content, but these do not show any correlation, indicating that F in biotite is not related to its $^{[6]}Al$ content (Munoz and Ludington, 1974).

Tables 4 and 8 and the X_{Mg} vs. F plot (Fig. 4d) show that F content of orthoamphibole is always lower than that of coexisting biotite (Fig. 4a), and the tables show that a large difference in F content exists between orthoamphiboles with similar X_{Mg} values from different hydrothermal veins. Table 4 and Figure 4d show that whenever a variation exists in the X_{Mg} of orthoamphiboles along a single vein, X_{Mg} increases when going from the vein

TABLE 8. Analyses of orthoamphibole along two hydrothermal veins described in this paper (G32 and G23) and hydrothermal subsilicic sodium gedrite (E7; Damman, 1988a)

	G32.01	G32.02	G23.3	G23.6	E7.27	E7.14
SiO_2	40.79	40.66	39.77	39.71	34.41	36.05
Al_2O_3	16.69	16.94	15.54	17.09	24.01	21.20
TiO_2	0.44	0.37	—	—	—	—
FeO	26.50	26.16	28.69	27.78	30.58	30.31
MnO	0.52	0.42	0.96	1.03	1.70	1.80
MgO	9.24	9.27	8.59	8.69	3.38	4.49
CaO	0.41	0.48	0.36	0.38	—	0.08
Na_2O	2.53	2.57	2.78	3.01	2.31	2.63
Cl^-	0.02	0.02	0.03	0.04	0.06	0.04
F^-	0.21	0.24	1.17	0.89	0.57	0.58
Total	97.36	97.14	97.89	98.62	97.02	97.18
Si	6.21	6.20	6.19	6.09	5.43	5.69
$^{[4]}Al$	1.79	1.80	1.81	1.91	2.57	2.31
$^{[6]}Al$	1.21	1.24	1.04	1.18	1.90	1.63
Ti	0.05	0.04	—	—	—	—
Fe	3.38	3.33	3.74	3.56	4.04	4.00
Mn	0.07	0.05	0.13	0.13	0.23	0.24
Mg	2.10	2.11	1.99	1.99	0.80	1.05
Ca	0.07	0.08	0.06	0.06	—	0.01
Na	0.75	0.76	0.84	0.90	0.71	0.80
Cl	0.01	0.01	0.01	0.01	0.02	0.01
F	0.10	0.11	0.57	0.44	0.28	0.29
Total	15.74	15.73	16.38	16.27	15.98	16.03
^{A}Na	0.63	0.62	0.80	0.82	0.68	0.73
X_{Mg}	0.38	0.39	0.35	0.36	0.16	0.21
$^{A}Na/^{[4]}Al$	0.35	0.34	0.44	0.43	0.26	0.32
Ed/Ts	0.54	0.53	0.79	0.75	0.36	0.46

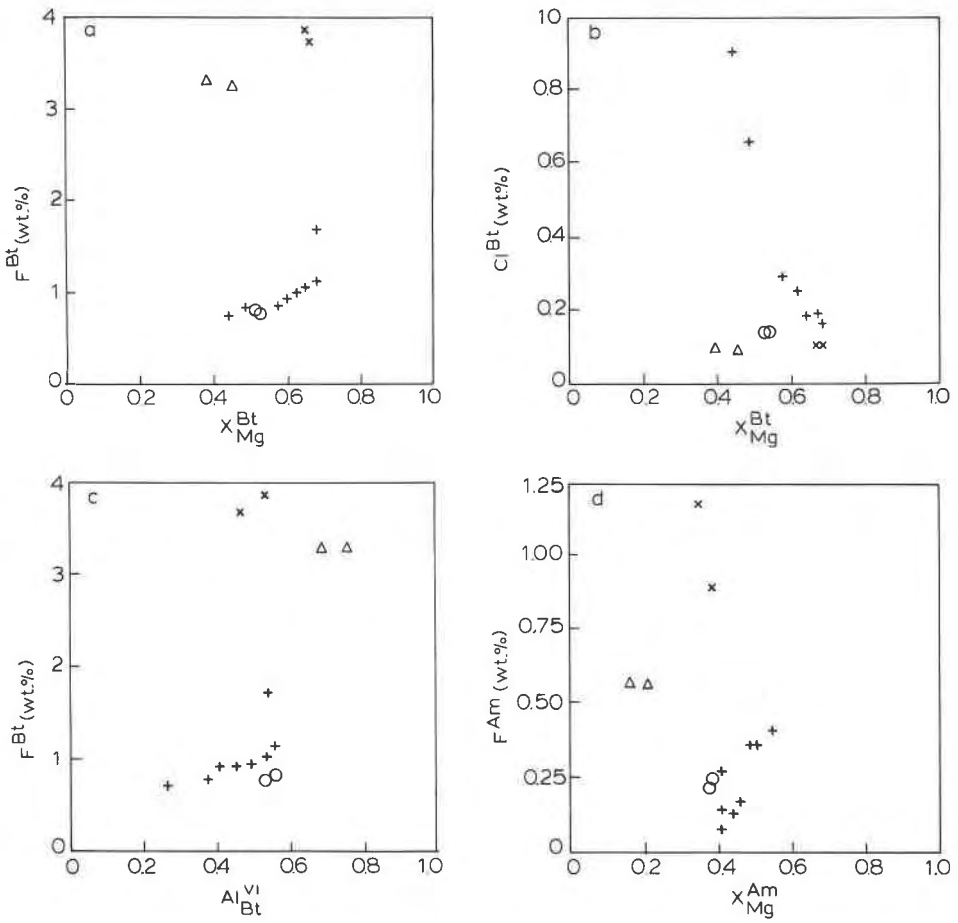

Fig. 4. (**a**) X_{Mg} vs. F, (**b**) X_{Mg} vs. Cl, (**c**) $^{[6]}$Al vs. F of biotite, and (**d**) X_{Mg} vs. F of orthoamphibole in and around hydrothermal veins associated with the Ostra Höjden granite. Each symbol represents one hydrothermal vein; + = da G11, see Tables 4 and 5; o = da G32, see analyses 1 and 2, Tables 7 and 8; × = da G23, see analyses 3 and 4, Tables 7 and 8; △ = da E7, see analyses 5 and 6, Tables 7 and 8 and Damman, 1988a. For errors in analyzed values, see Table 1.

outward, and the F content of the orthoamphiboles increases with increasing X_{Mg}. The above data suggests that, similar to biotite, the incorporation of F in orthoamphibole is controlled between veins by differences in f'_{HF} and, secondarily, along each vein at constant f'_{HF}, by the X_{Mg} of the orthoamphiboles (Berg, 1985).

A plot of X_{Mg} vs. Cl for the orthoamphiboles is not presented, because Cl in the orthoamphiboles rarely exceeds 0.05 wt% Cl (Tables 4 and 8).

Distribution of elements between coexisting orthoamphibole and biotite

The discussion of Figures 4a–4d shows that local variations of F and Cl fugacities are the most important control of the incorporation of these elements in orthoamphibole and biotite. A comparison of data from Tables 5 and 7 and Figure 5a shows that the difference between F contents of biotite and coexisting orthoamphibole ($F_{Bt} - F_{Am}$) increases with increasing f'_{HF} of the fluid with which they equilibrated, suggesting that an increase in f'_{HF} favors the incorporation of F in biotite over coexisting orthoamphibole. The ratio X^{Bt}_{Mg}/X^{Am}_{Mg} increases with increasing amounts of F in orthoamphiboles and biotite, expressed by F_{Bt} (Fig. 5b), indicating that the distribution of Mg and Fe between coexisting orthoamphibole and biotite is controlled by the F contents of these minerals, which in turn are governed by local variations in the F fugacity of the fluid with which they equilibrated (Tables 5 and 7).

→

Fig. 5. Distribution of elements between coexisting orthoamphibole and biotite: (**a**) $\log f'_{HF}$ vs. $(F_{Bt} - F_{Am})$; (**b**) F_{Bt} vs. $(X^{Bt}_{Mg}/X^{Am}_{Mg})$; (**c**) $\log f'_{HCl}$ vs. $(Cl_{Bt} - Cl_{Am})$; (**d**) Cl_{Bt} vs. $(X^{Bt}_{Mg}/X^{Am}_{Mg})$; (**e**) Ba_{Bt} vs. Cl_{Bt}; (**f**) Ti_{Bt} vs. Ti_{Am}; (**g**) Ti_{Bt} vs. Cl_{Bt}; (**h**) Mn_{Bt} vs. Mn_{Am}. For errors in analyzed values, see Table 1.

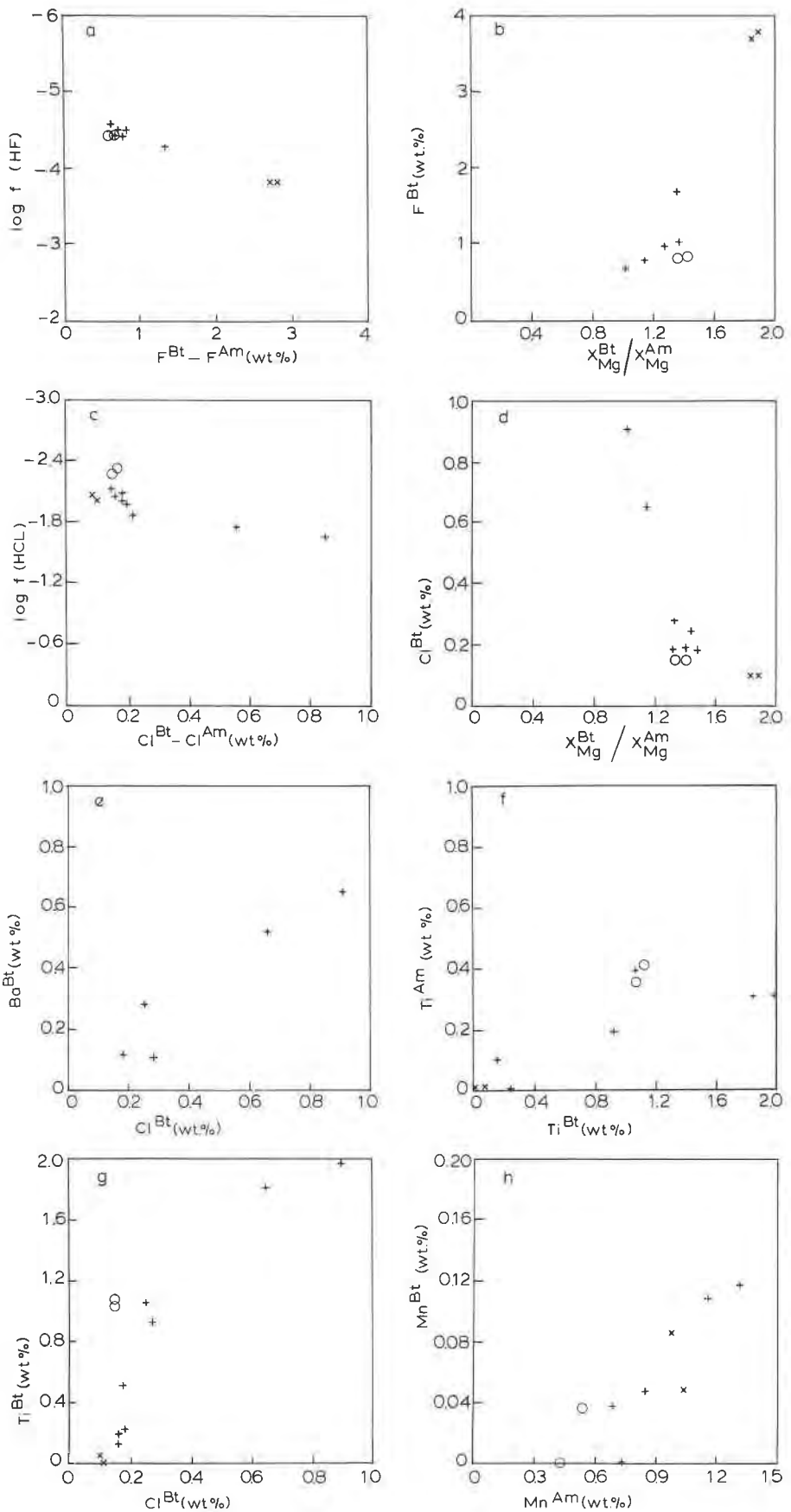
a
log f (HF)
$F^{Bt} - F^{Am}$ (wt%)
b
F^{Bt} (wt%)
$X^{Bt}_{Mg} / X^{Am}_{Mg}$
c
log f (HCL)
$Cl^{Bt} - Cl^{Am}$ (wt%)
d
Cl^{Bt} (wt%)
$X^{Bt}_{Mg} / X^{Am}_{Mg}$
e
Ba^{Bt} (wt%)
Cl^{Bt} (wt%)
f
Ti^{Am} (wt%)
Ti^{Bt} (wt%)
g
Ti^{Bt} (wt%)
Cl^{Bt} (wt%)
h
Mn^{Bt} (wt%)
Mn^{Am} (wt%)

The subsilicic sodium gedrite described by Damman (1988a) is omitted, becuase the crystallization sequence of this vein shows that its subsilicic sodium gedrite and biotite were not formed in equilibrium with one another. A comparison of data from Tables 5 and 7 with Figure 5c shows that the difference between the Cl contents of coexisting biotite and orthoamphibole ($Cl_{Bt} - Cl_{Am}$) increases with increasing f'_{HCl} in the fluid with which they equilibrated, suggesting that an increase in f'_{HCl} favors the incorporation of Cl in biotite over coexisting orthoamphibole. Only few biotites contain over 0.3 wt% Cl (Fig. 4b, Table 5); the coexisting orthoamphiboles never contain over 0.1 wt% Cl (Table 5). These Cl-rich biotites have relatively low F contents (Table 5). These biotites and coexisting orthoamphiboles show a decrease of X^{Bt}_{Mg}/X^{Am}_{Mg} with increasing Cl contents in both minerals, expressed by Cl_{Bt} (Fig. 5d). The above data indicate that the distribution of Mg and Fe between coexisting orthoamphibole and biotite with low F/Cl ratios is controlled by the amount of Cl in biotite, whereas with higher F/Cl ratios, the distribution of F between biotite and orthoamphibole is the most important controlling factor.

The biotites presented in Table 5 (group shown by + signs, Figs. 4a–4c) show a positive correlation between Ba and Cl (Fig. 5e); biotites along other veins are less Cl-rich (Fig. 4b) and do not contain more than 0.05 wt% Ba. Coexisting orthoamphiboles do not contain any Ba (Table 4), indicating that (1) Ba is preferentially incorporated in biotite over coexisting orthoamphibole and (2) an increase in f_{HCl} of fluids with which biotite equilibrated (Tables 5 and 7) enhances the incorporation of Ba in biotite. The Ti content of biotite is always higher than that of coexisting orthoamphibole (Fig. 5f). In biotite, Ti shows a strong positive correlation with Cl (Fig. 5g), implying that (1) Ti is preferentially incorporated in biotite over coexisting orthoamphibole and (2) incorporation of Ti in biotite, similar to incorporation of Ba, is enhanced by an increase in f'_{HCl} in the fluid with which the biotite equilibrated.

The Mn content of orthoamphibole is always higher than that of coexisting biotite (Fig. 5h), but there is no correlation with the Cl or F contents of the orthoamphiboles (Tables 4 and 8), indicating that (1) Mn is preferentially incorporated in orthoamphibole over coexisting biotite and (2) the incorporation of Mn in orthoamphibole is independent of variations in f'_{HF} and f'_{HCl} of the fluid with which the orthoamphibole equilibrated.

Acknowledgments

I would like to thank Prof. Dr. I. S. Oen and Drs. P. Maaskant, F. Spear, J. Munoz, K. Linthout, W. Lustenhouwer, and A. Boudreau for their help and encouragement during the preparation of this paper. Electron-microprobe analyses were performed at the electron-microprobe laboratory of the Instituut voor Aardwetenschappen, Vrye Universiteit, Amsterdam, with financial and personnel support of Z.W.O.-W.A.C.O.M. (research group for analytical chemistry of minerals and rocks subsidized by the Netherlands Organization for the Advancement of Pure Research).

References cited

Åberg, G., Bollmark, B., Björk, L., and Wiklander, U. (1983a) Radiometric dating of the Horrsjö granite, south-central Sweden. Geologiska Förenings i Stockholm Förhandlingar, 105, 78–81.

Åberg, G., Levi, B., and Frederiksson, G. (1983b) Zircon ages of metavolcanic and synorogenic granites from the Svardsjö and Yxsjöberg areas, south-central Sweden. Geologiska Förenings i Stockholm Förhandlingar, 105, 199–203.

Abraham, K., and Schreyer, W. (1973) Petrology of a ferruginous hornfels from Riegensgluck, Harz Mountains, Germany. Contributions to Mineralogy and Petrology, 40, 275–292.

Akella, J., and Winkler, H.G.F. (1966) Orthorhombic amphibole in some metamorphic reactions. Contributions to Mineralogy and Petrology, 2, 1–12.

Baker, J.H. (1985) The petrology and geochemistry of 1.9–1.8 Ga granitic magmatism and related sub-seafloor hydrothermal alteration and ore-forming processes. Ph.D. thesis, 204 p. University of Amsterdam. GUA Papers of Geology, Series 1, No. 21.

Berg, J.H. (1985) Compositional variation in sodium gedrite from Labrador. American Mineralogist, 70, 1205–1210.

Billström, K., Åberg, G., and Ohlander, B. (1988) Isotopic and geochemical data of the Pingstaberg Mo-bearing granite in Bergslagen, south-central Sweden. In J.H. Baker and R.H. Hellingwerf, Eds., The Bergslagen Province, central Sweden: Structure, stratigraphy and ore-forming processes—I.G.C.P. Project 247. Geologie en Mijnbouw, 67, 255–263.

Crowley, P.D., and Spear, F.S. (1981) The orthoamphibole volus: *P, T, X*(Fe-Mg). Geological Society of America Abstracts with Programs, 13, 435.

Damman, A.H. (1988a) Hydrothermal subsilicic sodium gedrite from the Gåsborn area, West Bergslagen, central Sweden. Mineralogical Magazine, 52, 193–200.

——— (1988b) Exhalative-sedimentary manganiferous iron ores from the Gåsborn area, West Bergslagen, central Sweden. In J.H. Baker and R.H. Hellingwerf, Eds., The Bergslagen Province, central Sweden: Structure, stratigraphy and ore-forming processes—I.G.C.P. Project 247. Geologie en Mijnbouw, 67, 433–442.

Guidotti, C.V. (1984) Micas in metamorphic rocks. Mineralogical Society of America Reviews in Mineralogy, 13, 357–468.

Helmers, H. (1984) Stages of granite intrusion and regional metamorphism in the Proterozoic rocks of western Bergslagen, central Sweden, as exemplified in the Grängen area. Neues Jahrbuch für Mineralogische Abhandlungen, 150, 307–324.

Jacobs, D.C. (1976) Geochemistry of biotite in the Santa Rita and Hannover-Fierro stocks, Central mining district, Grant County, New Mexico. Ph.D. dissertation, University of Utah, Salt Lake City, Utah.

James, R.A., Grieve, R.A.F., and Paul, L. (1978) The petrology of cordierite-anthophyllite gneisses and associated mafic and pelitic gneisses at Manitouwadge, Ontario. American Journal of Science, 278, 41–63.

Kroonenberg, S.B. (1976) Amphibolite-facies and granulite-facies metamorphism in the Coeroeni-Lucie area, southwestern Surinam. Ph.D. thesis, 259 p. University of Amsterdam, Amsterdam, Netherlands.

Lal, R.K., and Moorehouse, W.W. (1969) Cordierite-gedrite rocks and associated gneisses at Fishtail Lake, Harcourt Township, Ontario. Canadian Journal of Earth Sciences, 6, 145–165.

Leake, B.E. (1978) Nomenclature of amphiboles. American Mineralogist, 63, 1023–1053.

Leelanandem, C. (1969) H_2O^+, F, and Cl in the charnockitic biotites from Kondapalli, India. Neues Jahrbuch für Mineralogie Monatshefte, 461–468.

Magnusson, N.H. (1930) Långbans malmtrakt. Sveriges Geologiska Undersökning, ser. Ca, 23, 111 p.

Munoz, J.L. (1984) F-OH and Cl-OH exchange in micas with application to hydrothermal ore deposits. Mineralogical Society of America Reviews in Mineralogy, 13, 469–491.

Munoz, J.L., and Ludington, S.D. (1974) Fluoride-hydroxyl exchange in biotite. American Journal of Science, 274, 396–413.

——— (1977) Fluorine-hydroxyl exchange in synthetic muscovite and its

applications to muscovite-biotite assemblages. American Mineralogist, 62, 304–308.

Oen, I.S., Helmers, H., Verschure, R.H., and Wiklander, U. (1982) Ore-deposition in a Proterozoic incipient rift environment: A tentative model for the Filipstad-Grythyttan-Hjulsjö region, Bergslagen, Sweden. Geologische Rundschau, 71, 182–94.

Oen, I.S., Verschure, R., and Wiklander, U. (1984) Isotopic age determinations in Bergslagen: V. The Horrsjö granite. Geologie en Mijnbouw, 63, 85–88.

Otten, M.T. (1984) Na-Al–rich hornblende coexisting with hornblende in a corona between plagioclase and olivine. American Mineralogist, 69, 458–464.

Petersen, E.U., Essene, E.J., and Peacor, D.R. (1982) Fluorine end-member micas and amphiboles. American Mineralogist, 67, 538–544.

Robinson, Peter, Klein, C., and Ross, M. (1969) Equilibrium coexistence of three amphiboles. Contributions to Mineralogy and Petrology, 22, 248–258.

Robinson, Peter, Ross, M., and Jaffe, H.W. (1970) The composition field of anthophyllite and the anthophyllite miscibillity gap (abs.). American Mineralogist, 55, 307–309.

——— (1971) Composition of the anthophyllite-gedrite series, comparisons of gedrite-hornblende, and the anthophyllite-gedrite solvus. American Mineralogist, 56, 1005–1041.

Robinson, Peter, Spear, F.S., Schumacher, J.C., Laird, J., Klein, C., Evans, E.W., and Doolan, B.L. (1982) Phase relations of metamorphic amphiboles: Natural occurrence and theory. Mineralogical Society of America Reviews in Mineralogy, 9b, 1–228.

Ross, M., Papike, J.J., and Shaw, K.W. (1969) Exsolution textures in amphiboles as indicators of subsolidus thermal history. Mineralogical Society of America Special Paper 2, 275–299.

Spear, F.S. (1980) The gedrite-anthophyllite solvus and the composition limits of orthoamphibole from the Post Pond Volcanics, Vermont. American Mineralogist, 65, 1103–1118.

Valley, J.W., Petersen, E.U., Essene, E.J., and Bowman, J.R. (1982) Fluorphlogopite and fluortremolite in Adirondack marbles and calculated C-O-H-F compositions. American Mineralogist, 67, 545–557.

Volfinger, M., Robert, J.-L., Vielzeuf, D., and Neiva, A.M.R. (1985) Structural control on the chlorine content of OH-bearing silicates (micas and amphiboles). Geochimica et Cosmochimica Acta, 49, 37–48.

Zotov, I.A., and Siderenko, G.A. (1967) Magnesian gedrite from the southwestern Pamirs. Akademiya Nauk SSSR Doklady, 180, 138–141.

Manuscript received February 22, 1988
Manuscript accepted January 9, 1989